Journal of Harbin Engineering University
ISSN: 1006-7043

Vol 45 No. 8
August 2024

Design of DTC Controller for Three-phase Induction Motor

[1]Mohammed A. A. Elmaleeh, [2]Rihab Gafar Abdalla,
[1]Computer Engineering Department FCIT, Tabuk University, Tabuk, Saudi Arabia
[2]Faculty of Engineering, Aneelain University, Khartoum, Sudan

Abstract: Induction motors (IM) are among the most prevalently electric motors that are extensively utilized in industry. The control of these types of motors must be accurate and responsive to changes in torque and magnetic flux. Many induction motor control strategies have been introduced in recent years, direct torque control (DTC) is one of the most advanced types of induction motor control. This paper aims to design and improve the conventional torque control of induction motor using artificial neural networks. The main drawbacks of conventional torque control are high torque and flux ripples, variable switching behavior and control problems at low speeds. Artificial Neural Network (ANN) techniques are used to control the speed of induction motor and compared with the speed controller using proportional-integral-differential governor. The proposed models are implemented in MATLAB/SIMULINK platform which consists of subsystem models including induction motor, three-phase rectifier, three-phase inverter, along with the main controllers. The simulation results show a significant reduction in torque and flux ripples and improvements in the dynamic speed response.

Keywords: Induction motors (IM), Direct Torque control (DTC,), ANN

1. Introduction

IM are extensively used in industrial and profitmaking applications owing to their implicitly, efficiency, and roughness [1]. However, controlling these motors is a challenging task. Recently, various control strategies have been developed, including scalar control and vector control [2-4]. The scalar controller, which only manages the voltage's magnitude and frequency, is considered the simplest and easiest method for controlling IM [2-4]. However, to address issues of motor speed instability and significant torque and flux oscillations caused by the scalar controller, vector control has been adopted [5, 6]. Vector control is further divided into direct torque control (DTC) and field-oriented control (FOC) [5-7]. FOC mimics the dynamic response characteristics of a DC motor by indirectly controlling both torque and flux in IM applications. Despite this advantage, FOC requires many transformations, making its implementation more complex [8].

DTC, on the other hand, provides direct control of torque and flux in a two-level inverter without needing variable decomposition. This method allows for a quick dynamic response because torque and flux are directly controlled through voltage vectors chosen from a switching table. However, the hysteresis control method used in DTC can produce large torque and flux ripples. The basic configuration of DTC includes hysteresis control units for torque and magnetic flux, as well as a switching table. DTC is fundamentally simple in both function and concept, maintaining flux and torque within a narrow hysteresis band around their desired values. To achieve proper voltage vector selection, DTC uses a switching table that responds to variations in torque and stator flux [9-10].

DTC has become widely recognized as a high performance control strategy for variable speed alternating current (AC) drives and has attracted increased attention for industrial drive applications. The main impediment of induction machines resides in their speed control. The speed control of an induction machine signifies varying the AC voltage supply, the frequency of the supply, or both of them. The Conventional of Direct Torque Control is one of the stellar control strategy to control the speed and torque of induction motors. Nevertheless, the blemishes of the conventional DTC, instance of big torque and flux ripples and changing switching frequency handicap its implementation in AC drives especially at low speed. The main objectives of this research include to design a conventional direct torque control for induction motor using PID speed controller and to develop a

conventional direct torque control design by using intelligent systems such as neural networks with PID speed controller. Thereafter, using intelligent systems like neuro-fuzzy and neural network as a speed controller, that to have a highly response and overcome the ripples [9-10]

2. Direct Torque Control System Model

Utilizing the direct torque control is one of the best ways to control induction motors. The stator voltage vectors are selected in accordance to the variation of reference, and actual torque and stator flux. At this point, merely the stator currents and voltages are needed to determine the real torque and flux linkages. The torque state and flux's linkages is applied to obtain optimal switching logics, which are used for the switching of the three-phase inverter, Figure.1 illustrates a DTC control scheme in an unpretentious way [11-12].

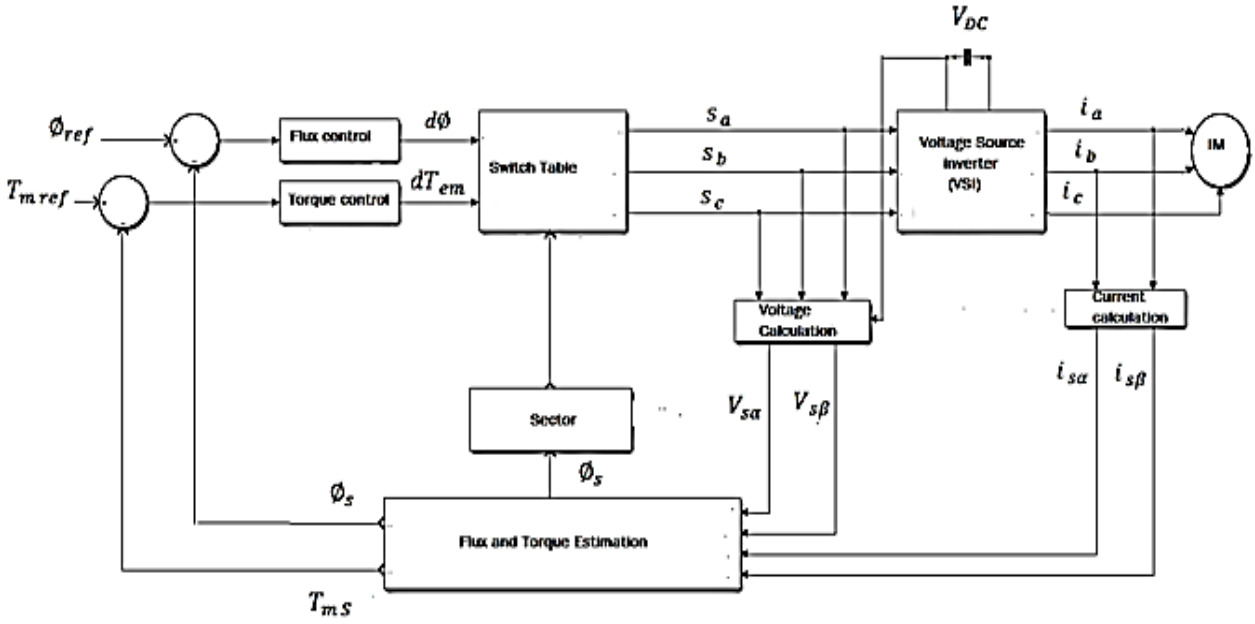

Figure1: The Block Diagram of DTC Model Scheme of IM [12]

2.1 Torque and Flux Hysteresis Comparators

The hysteresis comparisons are used to compare the torque and the flux to the corresponding reference values, in order to maintain a very close relationship with the reference values. For the flux, the hysteresis is at two levels [0, 1] while, for the torque, there are three levels, [-1, 0, 1]. These levels can be explained in the following equations [12]:

Case1: $|dT_e|$=1, If $|T_e|<|T_{e.ref}|-|\Delta T_e|$ (1)

Case 2: $|dT_e|$=0, If $|T_{e.ref}|-|\Delta T_e| \le |\Delta T_e|+|T_{e.ref}|$ (2)

Case 3: $|dT_e|$=-1, If $|T_e|>|T_{e.ref}|-|\Delta T_e|$ (3)

Where, $\Delta T_e = T_{e.ref} - T_e$

The flux hysteresis controller has two cases described in equations 4 and 5:

Case 1: $|d\varphi_s|$=1, If $|\varphi_s|-|\varphi_{s.ref}|-|\Delta\varphi_s|$ (4)

Case2: $|d\varphi_s|$=0, If $|\varphi_s| \ge |\varphi_{s.ref}|+|\Delta\varphi_s|$ (5)

The hysteresis comparator and switching table block are used to select the appropriate voltage vector, based on the sector number S(i). Referring to Table1, the corresponding quantities are increased when there is an extreme hysteresis and the reverse is true. The synthesized voltage vectors are sent to the voltage source inverter (VSI) [2]. The outputs of the hysteresis comparators with stator flux sector, where the stator flux space vector is located, select an appropriate inverter voltage vector from the switching table (Table 1). The selected voltage vector will be applied to the induction motor at the end of the sample time.

Table 1: Inverter Voltage Vector Switching Table

H_φ	H_{Te}	S1	S2	S3	S4	S5	S6
1	1	V_2	V_3	V_4	V_5	V_6	V_1
	0	V_0	V_7	V_0	V_7	V_0	V_7
	-1	V_6	V_1	V_2	V_3	V_4	V_5
0	1	V_3	V_4	V_5	V_6	V_1	V_2
	0	V_7	V_0	V_0	V_7	V_7	V_0
	-1	V_5	V_6	V_1	V_2	V_3	V_4

It could be noted that: in Figure1 there are two different loop corresponding to the magnitude of the stator flux and the torque. The motor speed error is given to speed controller produces reference torque and the output of the flux and torque comparators are fed into the hysteresis flux and torque controller blocks respectively. The stator flux status and the torque status with the position of the stator flux are used as inputs to obtain the switching Table block (Table1). The DTC also requires the flux and torque estimations by means of two phases' current and state of inverter.

2.2 Voltage Source Inverter (VSI)

Generally, the inverter basic operation is to convert the DC signal to AC signal and this signal is applied to a squirrel cage induction motor. Here, a VSI is used to regulate the motor's speed through the frequency and the voltage, as it includes an input rectifier, a DC link and an output converter. The inverter consists of three terminals, each terminal containing two insulated gate bipolar junction transistor (IGBT) which act as semiconductor switches [10, 13].

3. Direct Torque Control Mathematical Model

The electromagnetic torque (T_e) and the stator flux (φ_s) are obtained from the following equations [12]:

$$\varphi_s = \sqrt{\varphi^2{}_{s\alpha} + \varphi^2{}_{s\beta}} \qquad (6)$$

$$T_e = p * \left(\varphi_{s\alpha}.i_{s\beta} - \varphi_{s\beta}.i_{s\alpha}\right) \qquad (7)$$

Where p represents the poles.

The stator flux (α, β) references are calculated from:

$$\varphi_{s\alpha} = \int_0^t (v_{s\alpha} - R_s.i_{s\alpha}).dt \qquad (8)$$

$$\varphi_{s\beta} = \int_0^t (v_{s\beta} - R_s.i_{s\beta}).dt \qquad (9)$$

The angle is:

$$\theta_s = tan^{-1}\left(\frac{\varphi_{s\beta}}{\varphi_{s\alpha}}\right) \qquad (10)$$

Then, by comparing the estimated values of electromagnetic torque and the stator flux with their respective reference values, the values obtained by the comparison process are used as input values for hysteresis comparisons [14].

4. The Speed Controller

The Proportional-Integral (PI) controller is the most commonly used technique for controlling the speed of industrial machines [15]. It controls the errors by referencing to a closed-loop control system, thus correctly setting the controlled quantities such as the speed, the torque, and the flux. Furthermore, it aids the control unit by letting for the modification and testing through the amendment of the gain values and the ability to control the modifications in the system response. Nonetheless, the PI controllers poorly perform in the case of non-linear systems and during the operation of induction motors at relatively low speed.

5. Simulation Model of Direct Torque Control for 3Φ Induction Motor

Table 2 illustrates the parameters and the corresponding values selected in designing of induction motor.

Table 2: The Parameter of the Induction motor

Parameter	**Values**
Stator Resistance (Rs)	3.32 *ohm*
Stator Inductance (Ls)	4.39 *mH*
Rotor Resistance (Rr)	2.11 *ohm*
Rotor Inductance (Lr)	4.39 *mH*
Magnetizing Inductance (Lm)	0.2373
Inertia (J)	0.01 $kg.m^2$
Frequency	50 *Hz*
Voltage (line-line)	400
Number of Poles	2

The proposed design of the system is shown in Figure2. It divided into various subsystem. Figurese 3,4 and 5 describe the torque and the flux estimation, the torque and flux hysteresis controllers, the DTC controller unit, and the switching table including the selection voltage vector respectively. These subsystems models are

designed on the basics of the mathematical equations of the direct torque method which previously mentioned. Some simplifications were made within the model. The real motor stator flux linkage and the stator flux linkage estimates are essentially calculated using the same parameters in the motor and the DTC models. Several errors could be introduced to the measurements of the current and voltage with simple multiplications. Also the motor inductances were kept constant for the entire operating range, likewise in the magnetic circuit saturations were not considered the model simulation. Furthermore, since there is no thermodynamically modeling in the Simulink model, so the resistances also remain constant. Table 3 illustrates the parameters and the corresponding values selected in the design of the induction motor.

Table 3: IM parameter values

Parameter Name	Parameter Value
Nominal Voltage	2200VA
Stator Resistance (Rs)	3.32 *ohm*
Stator Inductance (Ls)	4.39 *mH*
Rotor Resistance (Rr)	2.11 *ohm*
Rotor Inductance (Lr)	4.39 *mH*
Magnetizing Inductance (Lm)	0.2373
Inertia (J)	0.01 $kg.m^2$
Frequency	50 *Hz*
Voltage (line-line)	400
Number of Poles	2

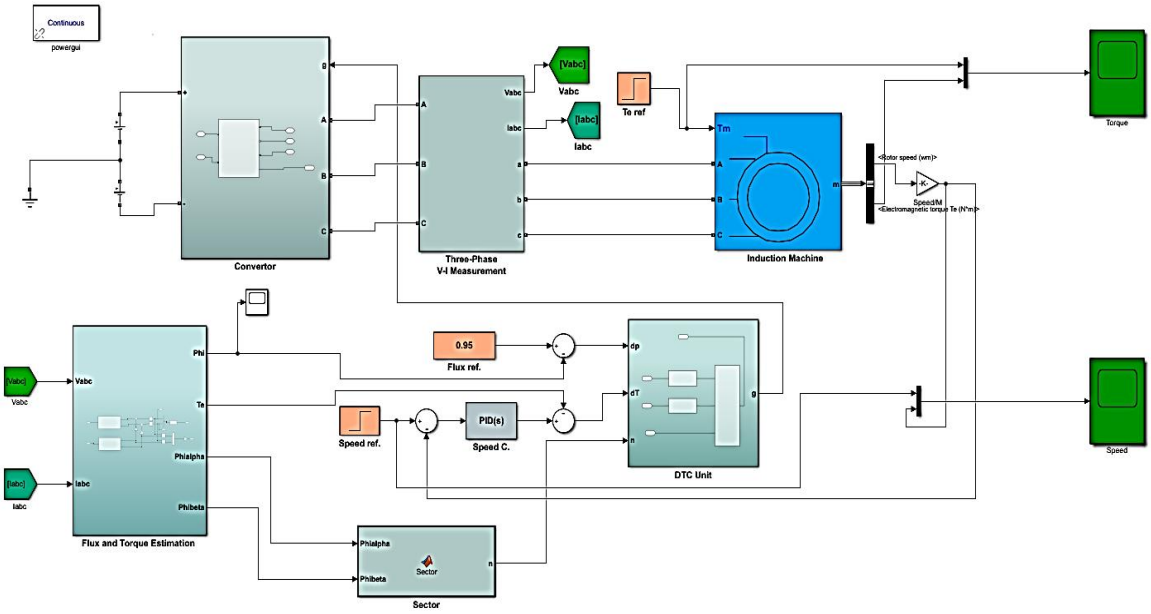

Figure2: The proposed System Simulation Diagram

Figure 3 includes the Flux and Torque Estimation. The flux hysteresis controller consists of two level controller, the stator flux error (ep) given to the flux controller and the flux error status (dp) (output) which has two values (0 or 1) [12].

$$ep = \varphi_{s.ref} - \varphi_s \qquad (11)$$

The stator flux controlled according to:

$|dp|$=1, If $|\varphi_s| \leq |\varphi_{s.ref}|$-$|ep|$, flux will be increased

$|dp|$=0, If $|\varphi_s| \geq |\varphi_{s.ref}|$+$|ep|$, flux will be decreased

Where:

$\varphi_{s.ref}$ ≡ the stator flux reference

The torque hysteresis controller shown in Figure4 has three output levels. The torque error (eT) which is given to the torque hysteresis controller, torque error status (dT) which represents the output with three values -1, 0 or 1 and the width of the hysteresis band (2eT) having the values (-1 to 0, 0 to 1).

$$\mathrm{eT} = T_{e.ref} - T_e \qquad (12)$$

$|dT|$=1, If $|T_e| < |T_{e.ref}|$-$|eT|$,

torque will be increased

$|dT_e|$=-1, If $|T_e|$> $|T_{e.ref}|$-$|eT|$,
torque will be decreased
$|dT_e|$=0, If $|T_{e.ref}|$- $|eT| \leq |Te| \leq |T_{e.ref}| + |eT|$,
torque will be remaining unchanged
Where:
$T_{e.ref}$ ≡ the torque reference

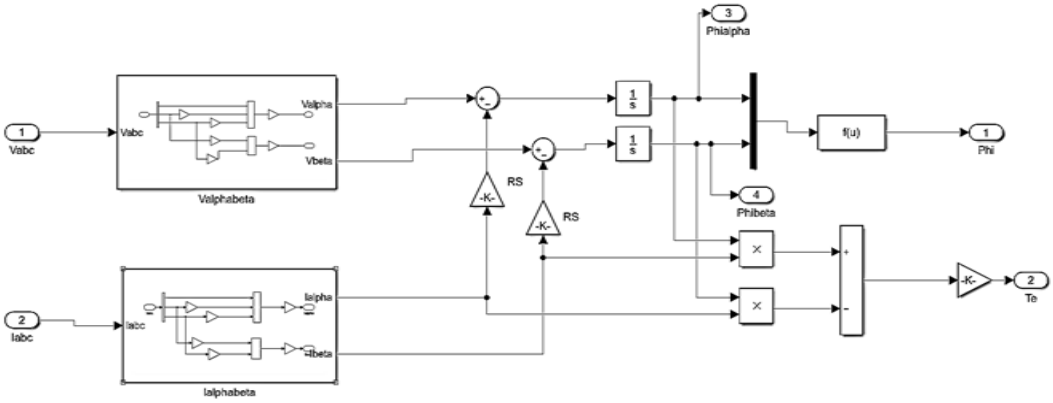

Figure 3: Flux and Torque Estimation

The DTC controller unit shown in Figurer4 consists of three inputs: the flux error status (dp), the torque error status (dT) and the sector number (n). As the stator flux estimate vector rotates around the origin it is necessary to know in which sector the stator flux vector is at any instant. As the stator flux estimate vector rotates around the origin, it is necessary to know the sector in which the stator flux vector is positioned at any given instant.

This allows selecting right states for the inverter switches as each of the six sectors has specified switch positions that adjust the stator flux vector and torque. (α-β)-plane is divided into six regions 60°apart from each other. The sector limits had been explained in Table 2.1. This inputs are given to the switching table for optimum voltage vector selection for the inverter gate

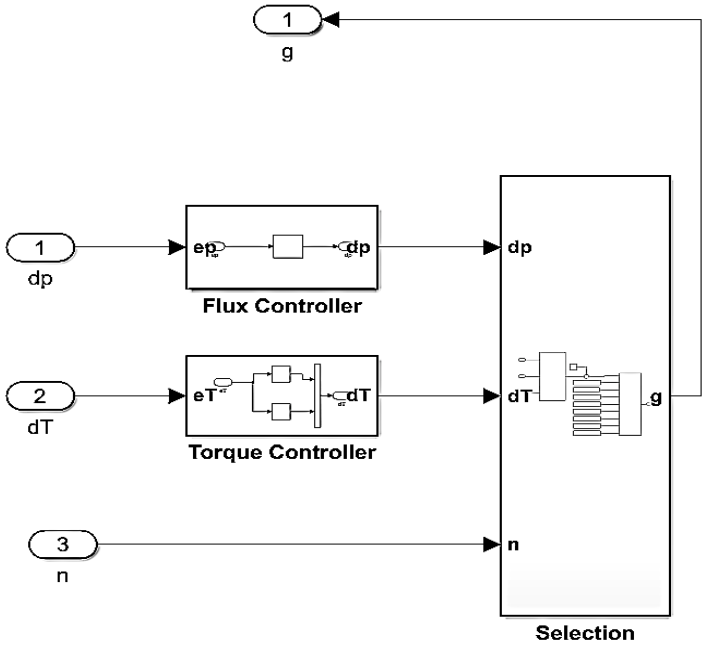

Fig.ure4: the DTC Control Unit

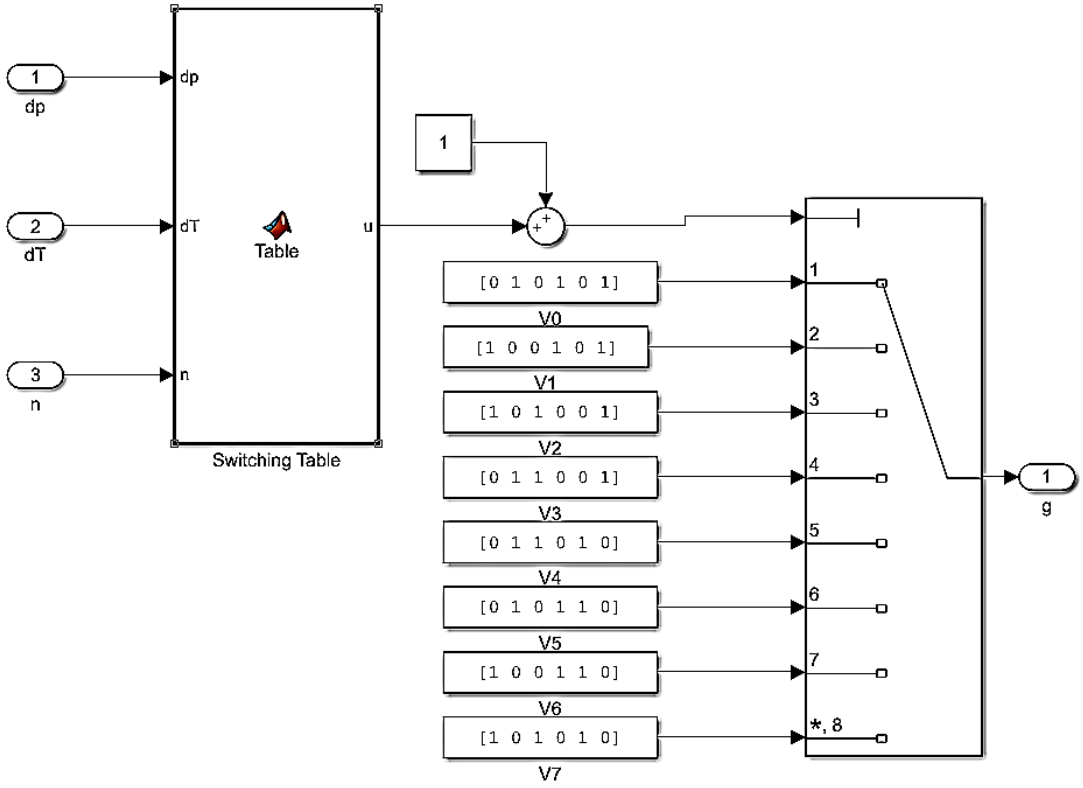

Figure5: Switching Table and Voltage Selector

The switching table logic is based on the outputs of the hysteresis controllers and sector table. The optimal switching table consists of six different switch position combinations for each of the six sectors. Switch states are based on eight voltage vectors (V_0 to V_7), where V_0 and V_7 are zero vectors. In this paper the MATLAB function block is used to obtain the optimal switching Table.

The high current, flux and torque ripple, complexity in torque and flux control at very low speed and slow transient response to the step change in torque through start-up are the disadvantages of CDTC based on hysteresis controllers. To enhance the system performance, most of the methods are used based on replacing the hysteresis with the non-hysteresis based controllers [17]. the intelligent techniques methods are utilized to improve the CDTC performance. These systems include: the include fuzzy logic, neural networks, nero-fuzzy and genetic algorithms [17]. Each of these intelligent methods enhanced the performance by making the adjustment to the comparator hysteresis or by replacement of the voltage vector selector beside the hysteresis using smart regulators.

In this design, neural network based on DTC will be used, the controller is used to substitute the switching Table, where the inputs are represented by the error of the flux, torque and the voltage sector. The output is represented by the pulses that control the inverter switching. Figure6 shows the simulation model of the artificial neural network DTC (ANNDTC) unit.

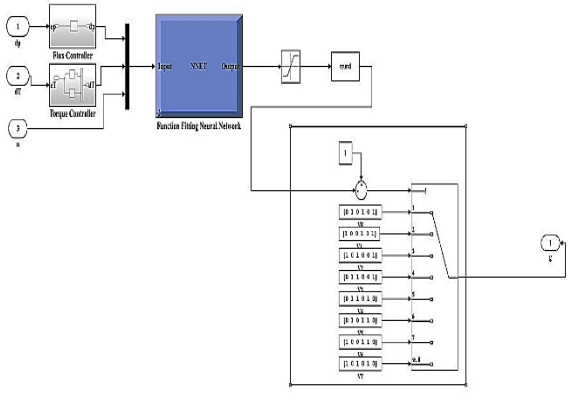

Figure6: The simulation model of the ANNDTC unit.

The neural network was designed to contain three inputs and one output. A number of different designs were tested in terms of the number of hidden layers and the number of neurons in all hidden layers. Based on the lowest error rate obtained, the neural network has been chosen. The proposed ANNDTC has been developed based on the conventional DTC technique. The proposed neural network DTC satisfies the parameters listed in Table4.

Table4: ANNDTC Parameters Using PID Speed Controller

PID Parameters	Value
k_p	150
k_i	0.5
k_d	0

5. Simulation Results

In Figure.3 the induction motor is powered by a VSI, which is built by combining Universal Bridge Blocks (UBBs). In order to create the torque and the flux references for the DTC unit, the speed loop-control defined to utilizing the PI controller. The motor torque and its flux are estimated and compared to their reference values through this control unit, which create comparators values, then, a switching table for producing an inverter switching pulses is produced by using the outputs of the comparators.

The dynamic and steady-state behavior of CDTC and ANNDTC drives, controlled by the proposed controllers, is investigated using MATLAB simulations. To compare the effectiveness of the PID speed controller with Neuro-Fuzzy and Neural Network controllers, all simulations are performed with the three controllers subjected to the same variations in load torque and reference speed.

The results of the simulation of the stator flux, electromagnetic torque, and speed control with a reference speed of 500 r.p.m using CDTC and ANNDTC with a PID speed controller are shown in Figures 7, 8 and 9 respectively.

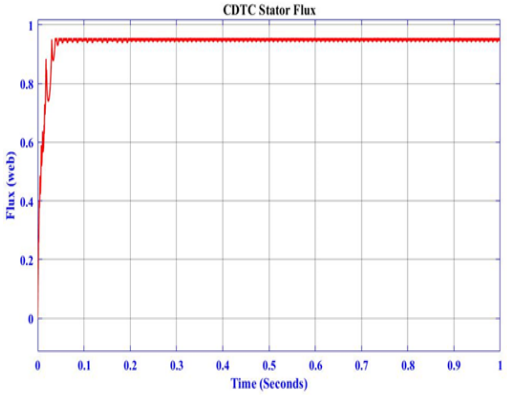

Figure7(a): Stator Flux Response of CDTC at speed of 500 rpm

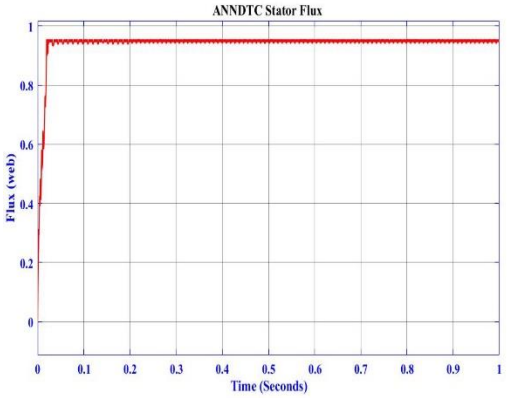

Figure7(b): Stator Flux Response of ANNDTC at speed of 500 4pm.

Figures 7(a) and 7(b) depict the stator flux responses for the CDTC and ANNDTC at motor speed of 500 rpm respectively. In Figure7(a), the flux ripple oscillates around the reference flux value which ranges between 1.075 and 0.825 Webs (this values were calculated from stator flux magnitude waveform by determining the difference between the maximum and minimum values). In contrast, Figure7(b) shows that the flux ripple is significantly reduced to ± 0.0168 Wb when using the ANNDTC. This marked reduction in flux ripple demonstrates the effectiveness of the ANNDTC approach. The simulation results reveal that the proposed scheme achieves a substantial decrease in flux ripples during the transient period when compared to the traditional CDTC method, highlighting the improved performance and stability offered by the ANNDTC controller.

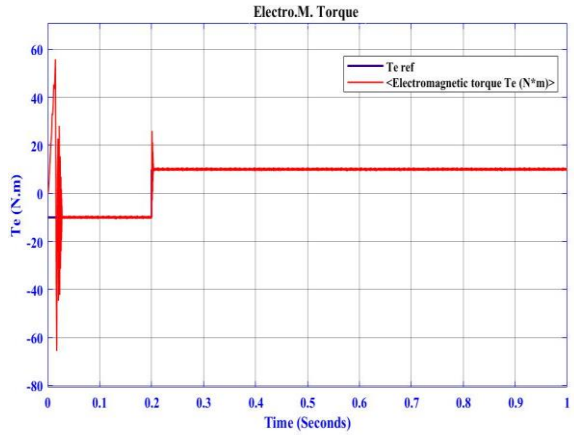

Figure 8(a): The Electromagnetic Torque Response of CDTC at speed of 500 rpm

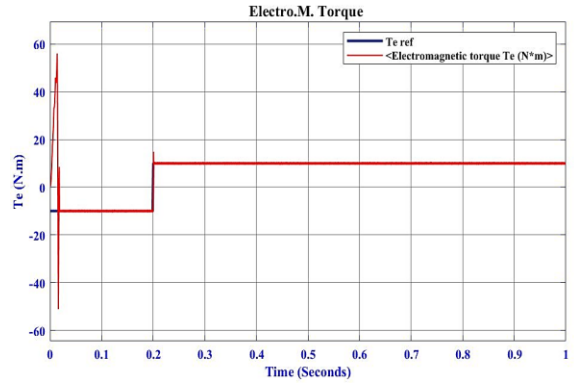

Figure 8(b): The Electromagnetic Torque Response of ANNDTC at speed of 500 rpm

Figures 8(a) and 8(b) depict the torque response during the transient period in CDTC and ANNDTC. The simulation results show considerable performance aberration with torque overshoot in the torque transient due to the hysteresis controllers used. The Torque Ripple Factor is defined as the ratio of the peak-to-peak torque ripple to the average torque. This dimensionless metric value quantifies the relative magnitude of the torque ripples (Peak-to-Peak Torque Ripple / Average Torque). The results show that the ANNDTC technique was able to reduce this torque ripple to 9.83%, down considerably from 16.1% in the case of CDTC. This demonstrates a 61% reduction in the torque ripple factor.

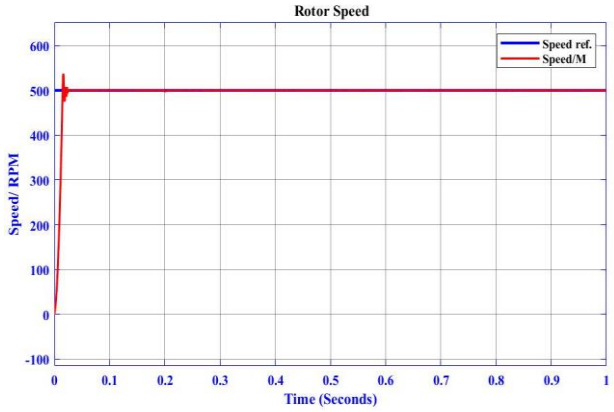

Figure 9(a): The Speed Response of CDTC with PID Controller

The speed response is shown in Figures 9(a) and 9(b), representing the performance of CDTC and ANNDTC. The speed response is shown in Figures 9(a) and 9(b),

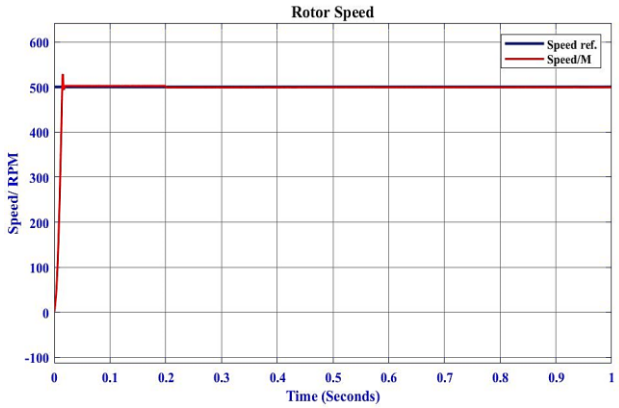

Figure9(b): The Speed Response of ANNDTC with PID Controller

representing the performance of CDTC and ANNDTC. Figure 9(a) reveals noticeable disturbances in the speed response, characterized by overshoots during the transient period and minor fluctuations in the steady state. Contrariwise, Figure 9(b) shows a significant decrease in both disturbances and overshoots compared to CDTC. This improvement is by reason of ANNDTC's ability to learn the complex nonlinear dynamics of the motor drive system, comprising the coupling between the torque, flux, and speed. This learning capability permits the ANNDTC to expect and recompense for the system's dynamic response, leading to a more optimal control of the speed during transients.

The simulations results have shown that ANNDTC can achieve faster speed response, reduced overshoot, and shorter settling times compared to conventional DTC, especially during the unexpected changes in the load or speed. Furthermore, Figure10 shows the speed response of both controllers at speed of 500 rpm.

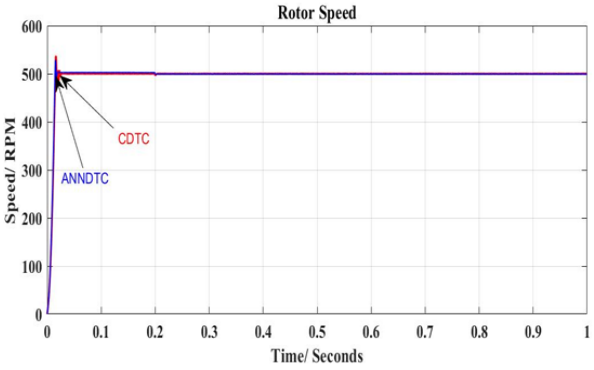

Figure10: Result of CDTC vs. ANNDTC Unit Using PID for Speed Controller

The specific characteristics and performance metrics of these control units are detailed in Table5. This comparison underscores the enhanced stability and precision of the ANNDTC, particularly in justifying transient overshoots and ensuring smoother steady-state operation.

Table5: Comparison between CDTC and ANNDTC Units

Parameter	CDTC	ANNDTC
k_p	150	150
k_i	0.5	0.5
k_d	0.01	0.01
Rise time /sec	0.0102	0.0096
Settling /sec	0.0220	0.0163
Overshoot (%)	7.8236%	5.9070%
Peak Time /sec	0.0168	0.0156
Torque Ripples (%)	16.1%	9.83%
Closed-loop stability	Stable	Stable

The results presented in Table 5 show that the k_p, k_i, and k_d have the same gains of 150, 0.5, and 0.01 for both CDTC and ANNDTC, respectively. This suggests that the primary difference between the two methods lies in the control strategy rather than the controller parameters. The performance metrics are deliberated as follows: Rise time: The ANNDTC method has a slightly faster rise time of 0.0096 seconds compared to 0.0102 seconds for the CDTC method. Settling time: The ANNDTC method has a significantly faster settling time of 0.0163 seconds compared to 0.0220 seconds for the CDTC method. Overshoot: The ANNDTC method has a lower overshoot of 5.9070% compared to 7.8236% for the CDTC method. Peak time: The ANNDTC method has a faster peak time of 0.0156 seconds compared to 0.0168 seconds for the CDTC method. Torque ripple: The ANNDTC method has a lower torque ripple of 9.83% compared to 16.1% for the CDTC method. In general, the comparison demonstrates that the ANNDTC method outperforms the CDTC method across multiple performance metrics, including faster rise time, settling time, lower overshoot, faster peak time, and reduced torque ripple. These improvements can be attributed to the artificial neural network-based control strategy employed in the ANNDTC method, which allows for more accurate modeling and control of the complex nonlinear system dynamics. The similar controller parameter values suggest that the primary difference between the two methods lies in the control algorithm itself, with the ANNDTC method providing superior torque control performance compared to the conventional CDTC approach.

Conclusion

This research paper affords a foundation for the work required to enable the successful design and control of induction motor speed using a DTC control system. The introduction covers the theoretical background of DTC and the control methods applied to induction motors. An effective DTC system design needs a stable mathematical model of the designated AC drives. The suitable control technique to be chosen always depends on the type of drive. Therefore, the paper concentrates on the conceptual design of the proposed system. First, it designs the CDTC using a PID speed controller, then designs the DTC based on ANN for choosing switching and uses an artificial intelligence speed controller such as ANN. The simulation results depict that the CDTC's drawbacks comprise torque and flux control difficulties at low speeds and more ripples in flux and torque. Nevertheless, the ANN control technique simulation results demonstrate substantial improvement in the

induction motor's performance regarding speed, electromagnetic torque, flux ripple, and speed responses in terms of ripple reduction.

References

[1] Jianguo, Song, and Chen Quanshi. "Research of electric vehicle IM controller based on space vector modulation direct torque control." 2005 International Conference on Electrical Machines and Systems. Vol. 2. IEEE, 2005.

[2] Takahashi, Isao, and Toshihiko Noguchi. "A new quick-response and high-efficiency control strategy of an induction motor." IEEE Transactions on Industry applications 5 (1986): 820-827.

[3] Kazmierkowski, Marian P., and Andrzej B. Kasprowicz. "Improved direct torque and flux vector control of PWM inverter-fed induction motor drives." IEEE Transactions on industrial electronics 42.4 (1995): 344-350.

[4] T. Noguchi, M. Yamamoto, S. Kondo, and I. Takashi, —High frequency switching operation of PWM inverter for direct torque, control of induction motor,‖ in Conference Record IEEE IAS Annual Meeting, 1997, pp. 775–780.

[5] Naik, N. Venkataramana, Aurobinda Panda, and Sajjan Pal Singh. "A three-level fuzzy-2 DTC of induction motor drive using SVPWM." IEEE Transactions on Industrial Electronics 63.3 (2015): 1467-1479.

[6] Vas, Peter. "Sensorless vector and direct torque control." (1998).

[7] Telford, Dwayne, Matthew W. Dunnigan, and Barry W. Williams. "A novel torque-ripple reduction strategy for direct torque control [of induction motor]." IEEE Transactions on Industrial Electronics 48.4 (2001): 867-870.

[8] Umanand, L., and S. R. Bhat. "Online estimation of stator resistance of an induction motor for speed control applications." IEE Proceedings-Electric Power Applications 142.2 (1995): 97-103.

[9] Dhanaselvam, J., et al. "Controlling of torque and flux for 3ϕ induction machine drive system (IMDS) using fuzzy controller (theory and introductory concepts)." 2017 IEEE International Conference on Power, Control, Signals and Instrumentation Engineering (ICPCSI). IEEE, 2017.

[10] Andreescu, Gheorghe-Daniel, et al. "Combined flux observer with signal injection enhancement for wide speed range sensorless direct torque control of IPMSM drives." IEEE Transactions on energy conversion 23.2 (2008): 393-402.

[11] Lascu, Cristian, Ion Boldea, and Frede Blaabjerg. "A modified direct torque control for induction motor sensorless drive." IEEE Transactions on industry applications 36.1 (2000): 122-130.

[12] Casadei, Domenico, et al. "FOC and DTC: two viable schemes for induction motors torque control." IEEE transactions on Power Electronics 17.5 (2002): 779-787.

[13] Baader, Uwe, Manfred Depenbrock, and Georg Gierse. "Direct self-control (DSC) of inverter-fed induction machine: A basis for speed control without speed measurement." IEEE transactions on industry applications 28.3 (1992): 581-588.

[14] Jonnala, Rohith Balaji, and Ch Sai Babu. "A Modified Multiband Hysteresis Controlled DTC of Induction Machine with 27-level asymmetrical CHB-MLI with NVC modulation." Ain Shams Engineering Journal 9.1 (2018): 15-29.

[15] Gadoue, Shady M., Damian Giaouris, and J. W. Finch. "Artificial intelligence-based speed control of DTC induction motor drives— A comparative study." Electric Power Systems Research 79.1 (2009): 210-219.

[16] Sudheer, H., S. F. Kodad, and B. Sarvesh. "Improved fuzzy logic based DTC of induction machine for wide range of speed control using AI based controllers." Journal of Electrical Systems 12.2 (2016): 301-314.

[17] Ponce, Pedro, Arturo Molina, and Arturo Tellez. "Neural network and fuzzy logic in a speed close loop for DTC induction motors." 2014 International Caribbean Conference on Devices, Circuits and Systems (ICCDCS). IEEE, 2014.